We are IntechOpen, the world's leading publisher of Open Access books Built by scientists, for scientists

4,800
Open access books available

122,000
International authors and editors

135M
Downloads

Our authors are among the

154
Countries delivered to

TOP 1%
most cited scientists

12.2%
Contributors from top 500 universities

CLARIVATE ANALYTICS
BOOK CITATION INDEX
INDEXED

WEB OF SCIENCE™

Selection of our books indexed in the Book Citation Index
in Web of Science™ Core Collection (BKCI)

Interested in publishing with us?
Contact book.department@intechopen.com

Zinc Oxide — Linen Fibrous Composites: Morphological, Structural, Chemical, Humidity Adsorptive and Thermal Barrier Attributes

Narcisa Vrinceanu, Alina Brindusa Petre,
Claudia Mihaela Hristodor, Eveline Popovici,
Aurel Pui, Diana Coman and Diana Tanasa

Additional information is available at the end of the chapter

1. Introduction

The augmented requirement for fibrous supports (yarns) possessing multifunctionality implies powerful emerging multidisciplinary approaches as well as the connection with the traditional scientific disciplines [1]. Finishing processes through nanoparticles were among the first commercial application in textiles domain.

Due to poor fixing of these nanoparticles on the textile surface, these finishes were not resistant to washing. Nanofinishings with improved bonding properties in fabrics and also impart desired wettability will result by using hydrophobic/hydrophilic functional polymer fibrous matrices as dispersion medium for nanoparticles.

Nanoparticles are extremely reactive, due to their high surface energy, and most systems undergo aggregation without protection of their surfaces. To eliminate or minimize generated waste and implement sustainable processes, recently green chemistry and chemical processes have been emphasized for the preparation of nanoparticles [2]. Much attention is now being focused on polysaccharides used as the protecting agents of nanoparticles. As stabilizing agent soluble starch has been selected and as the reducing agent in aqueous solution of $AgNO_3$ for silver nanoparticle growth, and a-D-glucose, has been elected. To maintain noble metal (platinum, palladium and silver) nanoparticles in colloid suspension, Arabinogalactan has been used as a novel protecting agent for [3]. Synthesized platinum, palladium and silver nanoparticles with narrow size distribution have been achieved by using porous cellulose

fibers as the stabilizer [4]. Pt nanoparticles can catalyze the carbonization of cellulose and mesoporous amorphous carbon is fabricated in high yields. The results are carbon-based functional composites with metal nanoparticles, showing that self-supporting macroporous sponges of silver, gold and copper oxide, as well as composites of silver/copper oxide or silver/titania can be routinely prepared by heating metal–salt-containing pastes of dextran, chosen as a soft template [5,6]. Polysaccharides could be used as stabilizer to synthesize nanoparticles of metal oxide and sulfides. Zinc oxide nanoparticles can be synthesized using water as a solvent and soluble starch as a stabilizer [7-9] while CdS nanoparticles have been prepared in a sago starch matrix.

In an earlier study, ZnO nanoparticles synthesis can be made with the assistance of MCT-β-CD (monochlorotriazinyl–β -cyclodextrin) by using a sol-gel method [10]. MCT-β-CD, a commercially available β- cyclodextrin with a reactive monochlorotriazinyl group, is used as a stabilizer. The so called anchor group reacting with cellulose hydroxyl radicals and cyclodextrin molecule is covalently bonded, to the fiber surface. The stable bound of cyclodextrin onto the textile fibers allows its properties to become intrinsic to the modified supports, thus a new generation of *intelligent textiles possessing* enhanced sorption abilities/capacities, as well as possessing active molecules release wasborn. Besides, as polysaccharide, MCT-β-CD shows interesting dynamic supramolecular associations facilitated both by inter- and intra-molecular hydrogen bonding, and polar groups. When a material is exposed to environmental water vapors, the water molecules firstly reacts with surface polar groups, forming a molecular monolayer.

Zinc oxide (ZnO), an n-type semiconductor, is a very interesting multifunctional material and has promising applications in solar cells, sensors, displays, gas sensors, varistors, piezoelectric devices, electro-acoustic transducers, photodiodes and UV light emitting devices. The adhesion between the ZnO nanoparticles and polymer through simple wet chemical method is rather poor and the nanoparticles may be removed from the host easily. In light of this, it is believed that the hydrothermal method can be a more promising way for fabricating nano-materials because it can be used to obtain products with modified morphological and chemical attributes with high purity, as well as stability in terms of water vapour sorption-desorption. Zn^{2+} ions can penetrate into the interior of linen fibrous support (fabric) easily when soluble salt such as zinc acetate ($Zn (OAC)_2$) is used. Reaction of Zn^{2+} ions leads to crystallization of ZnO nanoparticles within the linen fabric and to the formation of an encapsulated complex in the hydrothermal environment. The formation procedure can be described through two steps as shown in Fig. 1. Firstly, coordination compounds are formed through chelation between Zn^{2+} ions and the hydroxyl groups of linen fabric. Secondly, the in-situ crystallization of Zn chelate complex occurs under the hydrothermal treatment and forms a ZnO- coated linen fabric. The ZnO nanoparticles can thus be attached firmly within the linen fiber surface.

2. Advances in ZnO synthesis

The idea of the interaction of materials with water vapors is a new area of research. Almost all materials have some interaction with moisture that is present in their surroundings. The effects

of water can be both harmful and beneficial depending on the material and how it is used. Consequently, the point to determine a correlation between morphological, structural and chemical characterization and the water vapor sorption behavior of the analyzed samples has been emphasized. Consequently, the obtained textiles should find their applicability in textile processing industry subdomains, where a certain level of hydrophilicity/hydrophobicity is mandatory.

The main cause of polymeric materials degradation is the exposure to various factors such as: heat, UV light, irradiation ozone, mechanical stress and microbes. Degradation is promoted by oxygen, humidity and strain, and results in such flaws as brittleness, cracking, and fading [11-13]. There have been research reports targeting nanosized magnetic materials synthesis, having significant potential for many applications.

The applications of ZnO particles are numerous: varistors and other functional devices, reinforcement phase, wear resistant and anti-sliding phase in composites due to their high elastic modulus and strength. Otherwise, ZnO particles exist in anti-electrostatic or conductive phase due to their current characteristics. Few studies have been concerned with the application of ZnO nanoparticles in coatings system with multi-properties. The nano-coatings can be obtained by the traditional coatings technology, i.e., by filling with nanometer-scale materialsBy filling with nano-materials, both structure and functional properties of coatings can be modified. Super-hardness, wear resistant, heat resistance, corrosion resistance, and about function, anti-electrostatic, antibacterial, anti-UV and infrared radiation all or several of them can be realized.

Another idea this paper review was centered to was to study the thermal degradation behavior of some textile nanocomposites made of nano/micron particle grade zinc oxide and linen fibrous supports, and to discuss the thermal degradation mechanism of the above mentioned structures. There is also potential to highlight the effect of the functionalization agent - MCT-β-CD (monochlorotriazinyl–β–cyclodextrin) on the thermal stability and degradation mechanism of ZnO nanocoated linen fibrous samples.

In order to characterize the surface morphology and chemical composition of the treated supports, instrumental methods were conducted to measure the particle sizes of the reduced zinc oxide particles. The understanding of the thermal behavior of these fibers is very important since in general several conventional techniques used in textile processing industry, are conducted at high temperature.

The MCT-β-CD (monochlorotriazinyl–βeta-cyclodextrin) under the trade name CAVATEX or CAVASOL® W7 MCT (CAVATEX) from Wacker Chemie AG, $Zn(OAc)_2$, with an assay of 97%, urea and acetic acid (assay 99%) from CHIMOPAR, cetyltrimethylammonium bromide (CTAB) from Merck Company, with an assay of 97% were utilized

Two 100 % twill linen desized, scoured and bleached supports, each of size 3 cm × 3 cm were used as fibrous support. One of the supports has been coated with a certain concentration of MCT-β-CD (monochlorotriazinyl– β -cyclodextrin) [14-17].

Sample	Specifications
Reference 1	linen fibrous support
Reference 2	ZnO powder hydrothermally synthesized, non-calcinated
Sample 1	Functionalization of linen support with MCT- β –CD (**M**ono**C**hloro**T**riazinyl–**β** -**C**yclo**D**extrin) by exhaustion and thermal treatment
Sample 3	ZnO powder hydrothermally synthesized onto linen fibrous support
Sample 4	ZnO powder hydrothermally synthesized onto functionalized linen fibrous support
Sample 5	ZnO powder hydrothermally synthesized onto functionalized linen fibrous with the assistance of CTAB (Cetyl TrimethylAmmonium Bromide)
Sample 6	ZnO powder hydrothermally synthesized onto functionalized linen fibrous with the assistance of P123 (**M**ono**C**hloro**T**riazinyl-β – **C**yclo**D**extrin)
Sample 7	MCT- β –CD (**M**ono**C**hloro**T**riazinyl–**β** -**C**yclo**D**extrin)

Table 1. Synthesis conditions for each of the sample

2.1. Fundamental technique for synthesizing and characterizing nano-ZnO particles

The review was focused onto the fibrous supports (yarns) previously grafted/functionalized with MCT-β-CD. The grafting process of the textile fabric was performed following two other processes: the exhaustion and squeezing treatment and the heat treatment at 160°C. The purpose of these two treatments was the grafting the linen [18-20].

ZnO nanoparticles were synthesized *in-situ* on linen fibrous supports (yarns) having a certain concentration of MCT-β-CD by using the hydrothermal method. The linen samples with sizes of 30 x30 cm² were immersed in the solution prepared as follows: zinc acetate $Zn(CH_3COO)_2$. $2H_2O$, purity – 99%) (0,005 mol/1000mL) as precursor was solved in de-ionized water to form a uniform solution by stirring and then 0,1 mol of urea solution was added drop-wise with constant stirring. Second, the pH value of the mixed solution was adjusted to 5 by adding acetic acid drop wise. The final reaction mixture was then vigorously stirred for two hours at room temperature and poured into 100 mL stainless-steel autoclaves made of Teflon (poly[tetra-fluoroethylene), followed by immersion of the fibrous supports (yarns). Then the autoclaves were placed in the oven for the hydrothermal treatment at 90°C overnight. The autoclaves were then cooled down to room temperature. The treated fabrics were then removed from the autoclaves. The treated fabrics were washed several times with distilled water. After complete washing the composites were dried at 60∘C overnight for complete conversion of the remaining zinc hydroxide to zinc oxide
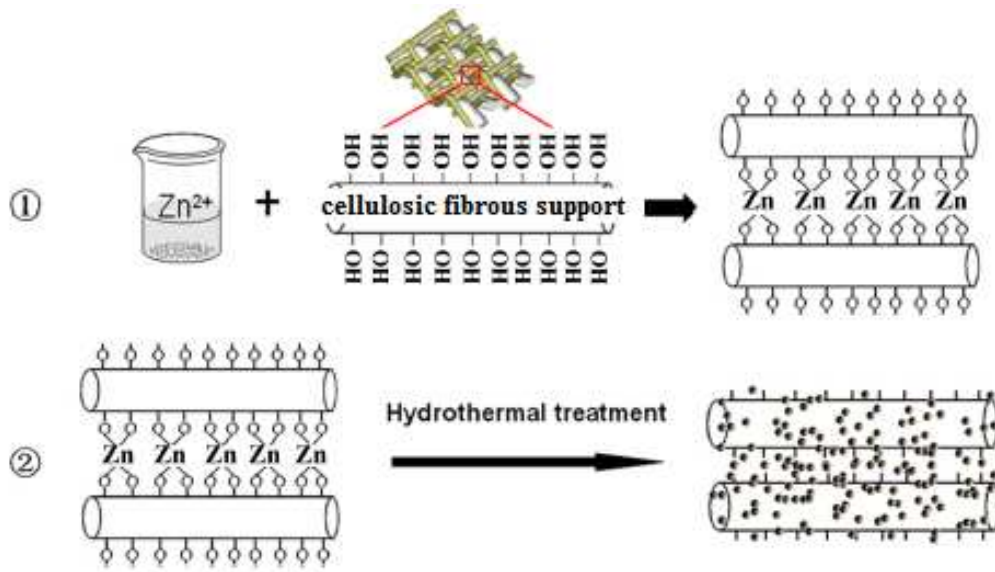
Figure 1. Flow chart for the preparation of nanoparticle coated linen support [10]

Thermal treatment relied into two main stages, into the calcination oven. Firstly, the samples were subjected to an increasing of temperature up to 150°C; secondly the probes were heated up to 350°, 450° respectively.

Scanning Electron Microscope (SEM) images were acquired with a Quanta 200 3D Dual Beam type microscope, from FEI Holland, coupled with an EDS analysis system manufactured by EDAX - AMETEK Holland equipped with a SDD type detector (silicon drift detector). Taking into account the sample type, the analyses have been performed, using Low Vacuum working mode, (as in High Vacuum working type). Both for the acquisition of secondary electrons images (SE – secondary electrons) and EDS type elemental chemical analyses, LFD (Large Field Detector) type detector was used, running at a pressure of 60 Pa, and a voltage of 30 kV.

The ZnO–MCT-β-CD treated fabrics were tightly packed into the sample holder. X-ray Diffraction (XRD) data for structural characterization of the various prepared samples of ZnO were collected on an X-ray diffractometer (PW1710) using Cu-Kα radiation (k = 1.54 Å) source (applied voltage 40 kV, current 40 mA). About 0.5 g of the dried particles were deposited as a randomly oriented powder onto a Plexiglass sample container, and the XRD patterns were recorded at 2θ angles between 20° and 80∘, with a scan rate of 1.5°/min. Radiation was detected with a proportional detector [21-25].

2.2. Evaluation of crystallinity

The extent of crystallinity (*Ic*) was estimated by means of Eq. (1), where I_{020} is the intensity of the 020 diffraction peak at 2θ angle close to 22.6°, representing the crystalline region of the material, and I_{am} is the minimum between 200 and 110 peaks at 2θ angle close to 18°, repre-

senting the amorphous region of the material in cellulose fibres [26-28]. I_{020} represents both crystalline and amorphous materials while I_{am} represents the amorphous material.

$$I_C = \frac{I_{020} - I_{am}}{I_{020}} x100(\%)$$ (1)

A *shape factor* is used in x-ray diffraction to correlate the size of sub-micrometre particles, or crystallites, in a solid to the broadening of a peak in a diffraction pattern. In the Scherrer equation,

$$\tau = \frac{K \bullet \lambda}{\beta \cos\theta}$$

where K is the shape factor, λ is the x-ray wavelength, β is the line broadening at half the maximum intensity (FWHM) in radians, and θ is the Bragg angle [29]. τ is the mean size of the ordered (crystalline) domains, which may be smaller or equal to the grain size. The dimensionless shape factor has a typical value of about 0.9, but varies with the actual shape of the crystallite.

FTIR was used to examine changes in the molecular structures of the samples. Analysis has been recorded on a FTIR JASCO 660+ spectrometer. The analysis of studied samples was performed at 2 cm^{-1} resolution in transmission mode. Typically, 64 scans were signal averaged to reduce spectral noise.

For the studied samples dynamic vapours sorption (DVS) capacity, at 25°C averaging in the domain of relative humidity (RH) 0-90% has been investigated by using an IGAsorp apparatus, a fully automated gravimetric analyzer, supplied by Hiden Analytical, Warrington - UK). It is a standard sorption equipment, which has a sensitive microbalance (resolution 1µg and capacity 200 mg), which continuously registers the weight of the sample in terms of relative humidity change, at a temperature kept constant by means of a thermostatically controlled water bath. The measuring system is controlled by appropriate software.

To study water sorption at atmospheric pressure, a humidified stream of gas is passed over the sample.

The differential scanning calorimetry analysis (DSC) of fibrous supports - ZnO composites were carried out using a NETZSCH DSC 200 F3 MAIA instrument under nitrogen. Initial sample weight was set as 30-50 mg for each operation. The specimen was heated from room temperature to 350°C at a heating rate of 10°C/min.

3. Prominent assessed features of fibrous composites

From the obtained images it was clearly distinguished the hexagonal shape of ZnO agglomerations and the morphology of linen fibres (Fig.2c).
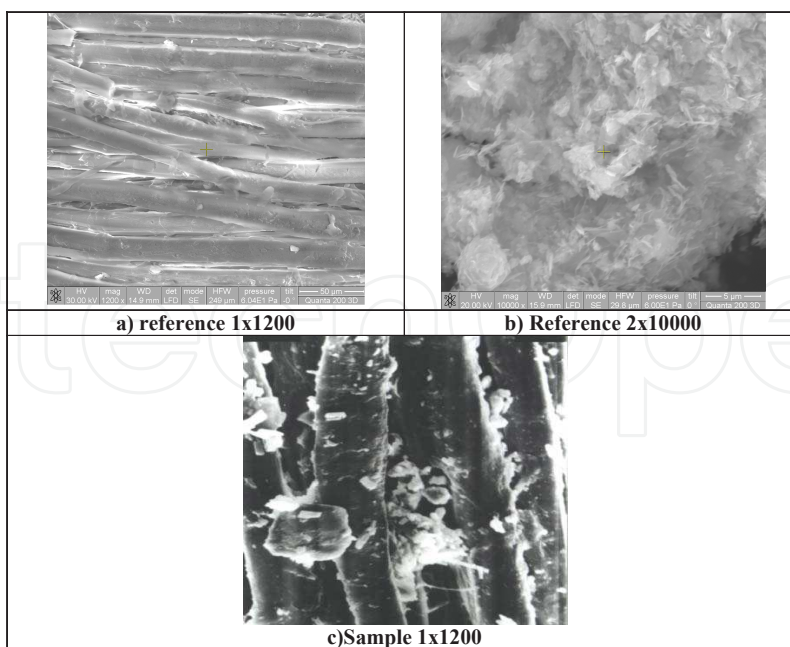
a) reference 1x1200

b) Reference 2x10000

c)Sample 1x1200

Figure 2. SEM images of: reference samples and of the functionalized linen support with MCT- β –CD sample [10]

x1270

x5000

a. Sample 6

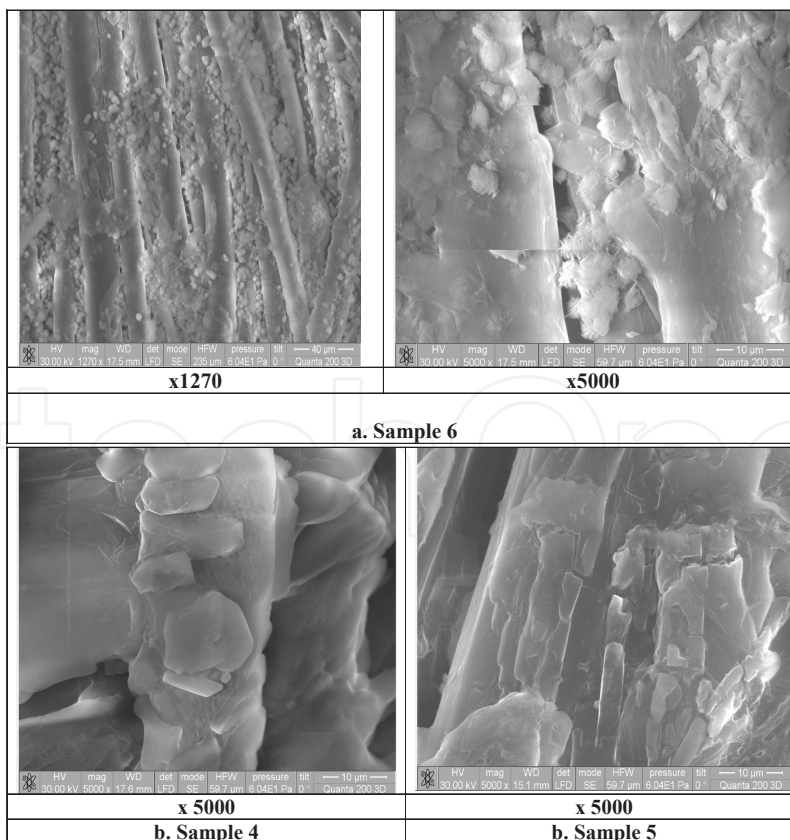**x 5000**

x 5000

b. Sample 4

b. Sample 5

Figure 3. images of some textile composites [10]

The SEM images of functionalized linen supports coated with ZnO with assistance of the studied surfactants (Fig 3 a and b) indicate different shapes of deposited ZnO.

On the other hand, ZnO nanoparticles exhibited hexagonal form like flowers of ZnO nano-crystals, if the treatment was assisted by P123 surfactant (Fig. 3 a) and lamellar morphology if the treatment was assisted by CTAB (Fig. 3 b) respectively.

The particles uniformly cover the fibrous support surface and as results, the fibrous supports surface became coarser after the treatment.

The adhesion strength of ZnO particles on fibrous support is different in terms of the applied surfactant treatment and was tested after repeated washing cycles (1 minute ten times).
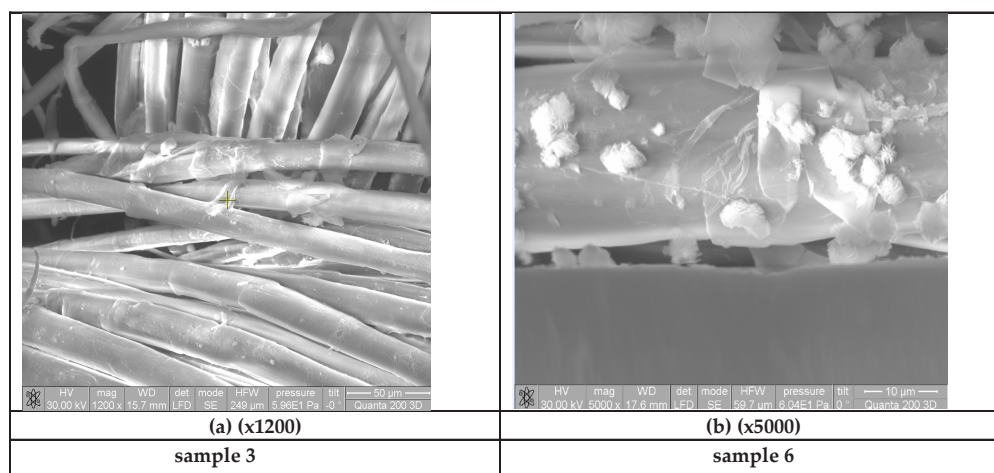

(a) (x1200)	(b) (x5000)
sample 3	sample 6

Figure 4. SEM images of some textile composites after repeated washing cycles [10]

According to the SEM images (Fig 4 a and b), the adhesion strength of ZnO powder hydro-thermally deposited onto functionalized linen fibrous support is superior in the case of functionalized surface (Fig 4 b) compared with the non-functionalized surface (Fig 4a). The functionalization advantage has been evaluated considering the durability of ZnO on the support surface after repeated cycles of washing. After washing the coating particles fell off easily for the ZnO powder hydrothermally synthesized without functionalization, which might have been caused by the weak attaching force.

As shown in Fig. 4, before treatment the diameters of fibrous supports (individual yarns) are about 10 - 20 μm; after treatment SEM image show very clearly the individual yarns, covered by various ZnO aggregates deposition.

3.1. Mechanistic aspect of nanoparticle formation

The shape and the manner of covering depend of linen grafting agent assistance. This result is correlated with the high number of coordinating functional groups (hydroxyl and glucoside groups) of the MCT-β-CD which can form complexes with divalent metal ions [15]. During the synthesis time, it might be possible that the majority of the zinc ions were closely associated with the MCT-β-CD molecules. Based on the previous research, it can be claimed that nucleation and initial crystal growth of ZnO may preferentially occur on MCT-β-CD [16]. Moreover, as polysaccharide, MCT-β-CD showed interesting dynamic supramolecular associations facilitated by inter- and intra-molecular hydrogen bonding, which could act as matrices for nanoparticle growth in size of about 30–40 nm. They aggregated to irregular ZnO–CMC nanoparticles in a further step (Figures 4a) and 4 b). In these figures, SEM images of linen supports coated with ZnO with assistance of the two surfactants show that the nanoparticles exhibited an approximately lamellar morphology and the particles can be seen to be coated on the fibrous support surface (yarn). As result, the fibrous supports (yarns) surface became coarser after the treatment.

In the case of CTAB assistance, on the yarns surfaces large ZnO particles, covering the yarn as a bark are noticeable (Fig. 3b), involving that the large particles may be formed via precipitation followed by a step-like aggregation process. In addition, according to the SEM images of the coated fabric, the uniformity of the fabric coated with ZnO powder hydrothermally synthesized with assistance of CTAB (Cetyl trimethylammonium bromide) is better than that of ZnO powder hydrothermally synthesized in the presence of Pluronic P123 and possesses good washing fastness. The last one has not been measured, but it has *apriori* been evaluated. This phenomenon can be explained by the fact that the repeated cycles of washing and rinsing did not conduct to the washing away of the ZnO particles; subsequently the zinc oxide proven a low extent of washing fastness. This statement is also in a good correlation with the XRD results, claiming a slight shift of ZnO intensity peaks, meaning that the nucleation of the zinc oxide occurred not only the support surface, but also within the nanocavities, due the fibers roughness.

In case of ZnO powder hydrothermally synthesized without any surfactant assistance, the coating particles fell off easily after washing, which might have been caused by the weak attaching force (coordinated bond between ZnO and linen) induced by the deteriorated crystallinity.

The SEM image of functionalized fabric support show very clearly the individual yarns, having diameters of about 10-20 μm, covered by various ZnO aggregates (Fig.4). MCT-β-CD can form complexes with divalent metal ions, due to its high number of coordinating functional groups (hydroxyl and glucoside groups) [31]. There is a possibility that the majority of the zinc ions were closely associated with the MCT-β-CD molecules. Based on the previous research, it can be claimed that nucleation and initial crystal growth of ZnO may preferentially occur on MCT-β-CD [32]. Moreover, as polysaccharide, MCT-β-CD showed interesting dynamic supramolecular associations facilitated by inter- and intra-molecular hydrogen bonding, which could act as matrices for nanoparticle growth in size of about 30–40 nm. They aggregated to irregular ZnO–CMC nanoparticles in a further step.

Element	Wt%	At%
CK	25.34	46.47
NK	15.45	24.30
OK	08.91	12.27
BrL	01.90	00.52
CaK	00.63	00.35
ZnK	47.77	16.10
Matrix	Correction	ZAF

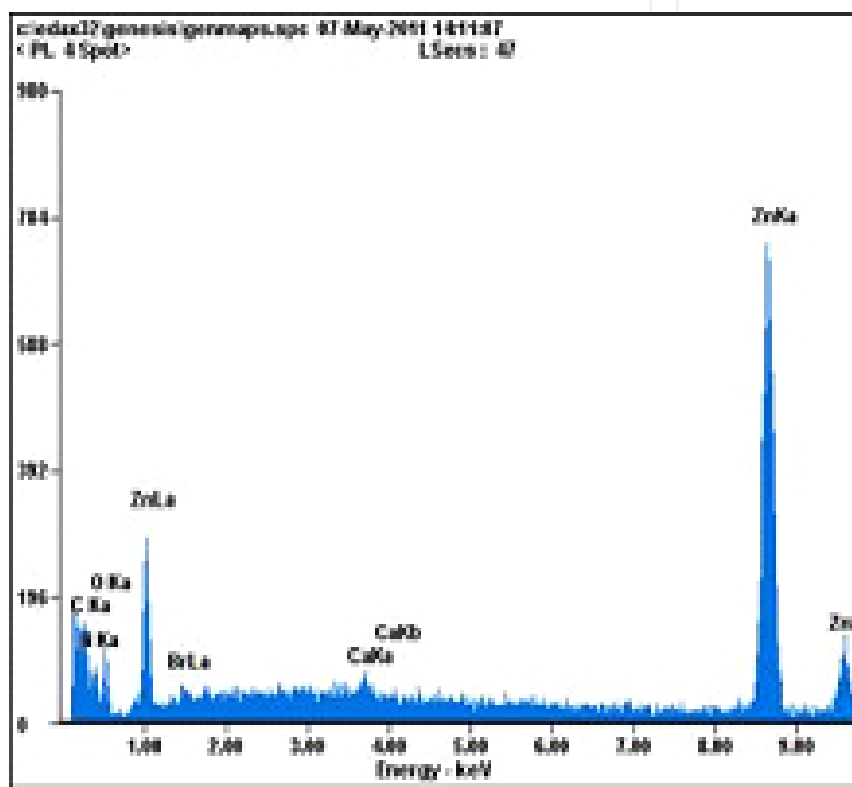**Table 2.** Surface composition from EDX measurements at sample 6

Figure 5. EDX analysis (sample 6) (Wt: weight percent, At: atomic percent). [10]

The outcome of the EDX elemental analysis for sample 6 illustrated in Figure 5 and Table 2, show that surface composition contain approximately 47% ZnO, meaning that ZnO phase represented almost half of the sample mass.

The X-ray diffraction patterns of samples 4-7 compared with reference 2 are represented in Fig. 6:

Figure 6 shows the selected-area diffraction pattern (2θ=20-40º) of the obtained samples. The obtained XRD pattern and indexed lines of ZnO (reference 2) are presented in Figure 6. According to the literature [33], all the diffraction lines are assigned to the wurtzite hexagonal phase structure.
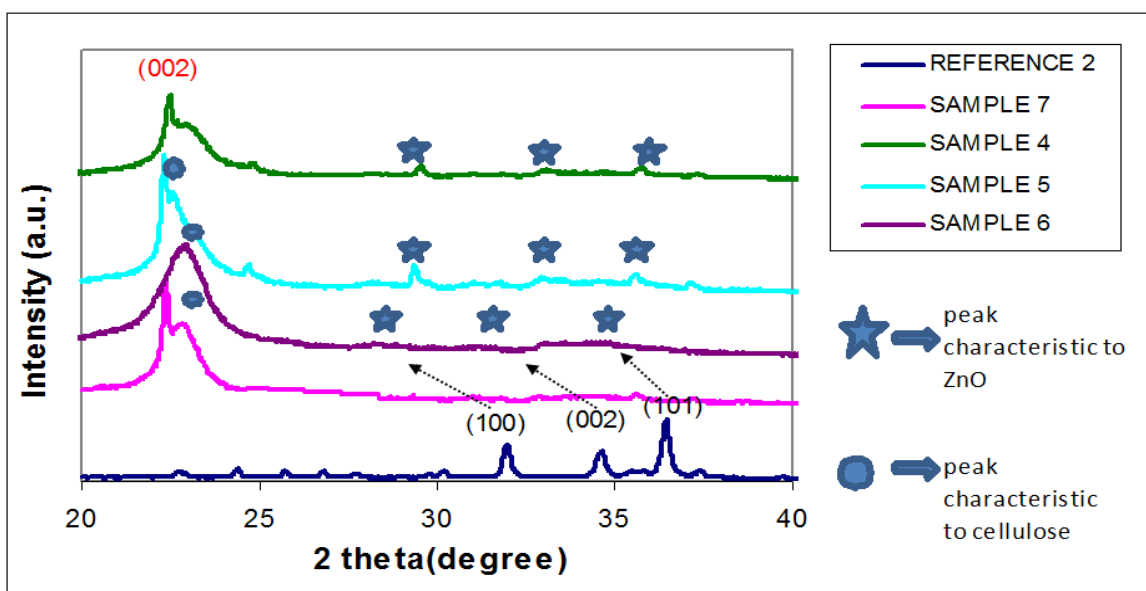
Figure 6. Color online) XRD patterns of: Reference 2; Sample 4; Sample 5; Sample 6; Sample 7[10] The arrows indicate the peaks shift, in terms of working conditions. The height of the peaks has been multiplied by a 40 factor.

The composites patterns (sample 3-6) reveal both the presence of the peaks positions that matched well with those of the ZnO XRD pattern - lines (100), (002) and (101) - and the main peak of cellulose - linen (002) [34]. The small relative intensity of the peaks of the ZnO–linen composites is not well correlated with the EDX analysis, which showed a high content of deposited ZnO. The observed ZnO diffraction lines shift (samples 4 and 5) denotes the fact that the growth of the ZnO takes place not only on the support surface, but also inside the nanocavities due to the fibers roughness.

The intensities of the diffraction peaks decrease when the synthesis takes place with the assistance of the surfactant, that prevent crystal growth in these working conditions (Fig.6).

In Fig. 7, the *FTIR spectrum* of hydrothermally synthesized, non-calcinated ZnO powder exhibited a high intensity broad band at about 430 cm^{-1} due to the stretching of the zinc and oxygen bond.

As shown in the FTIR spectrum of MCT-β-CD, the absorption bands between 1000 and 1200 cm^{-1} were characteristic of the – C –O– stretching on polysaccharide skeleton.A similar band was also observed in synthesized ZnO composites. And two peaks appeared at 1420 and 1610 cm^{-1} corresponding to the symmetrical and asymmetrical stretching vibrations of the carboxylate groups [35]. The peak at 2920 cm^{-1} was ascribed to C–H stretching associated with the ring methane hydrogen atoms. A broad band centered at 3450 cm^{-1} was attributed to a wide distribution of hydrogen-bonded hydroxyl groups. The FTIR spectra indicated that in ZnO–MCT-β-CD nanoparticles, there was the strong interaction, but no obvious formation of covalent bonds between MCT-β-CD) and ZnO.

Water vapors sorption behavior. Isothermal studies can be performed as a function of humidity (0-95%) in the temperature range 5° C to 85° C, with an accuracy of ± 1% for 0 - 90% RH and ±
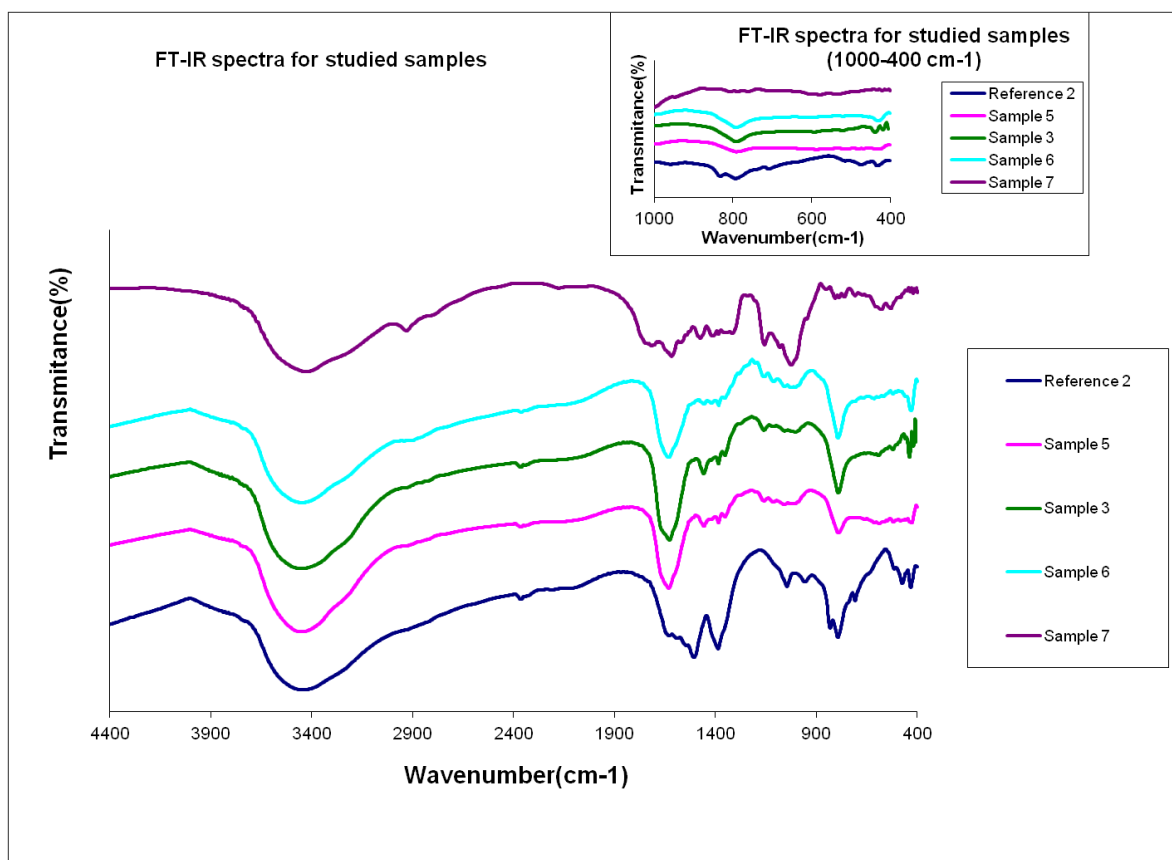
Figure 7. a) FTIR of spectra of: sample 3; sample 5; Sample 6 ; sample 7; Reference 2 [10]

2% for 90 - 95% RH. The relative humidity (RH) is controlled by wet and dry nitrogen flows around the sample. The RH is held constant until equilibrium or until a given time is exceeded, before changing the RH to the next level.

The vapours pressure in the sample room has been achieved by 10 steps of 10% humidity, each of them having a time of equilibrium setting between 10-20 minutes. At each phase, the weight adsorbed by the sample is measured by electromagnetic compensation between tare and sample, when the equilibrium is reached. Apparatus has an anti-condensation system for the cases that vapors pressure is very close/near to that of saturation. The cycle is finished by decreasing in steps of vapors pressure, in order to obtain desorption isotherms, as well.

Prior to measuring of sorption-desorption isotherms, drying of the samples is performed in nitrogen flow (250 mL/min) at 25°C, until the sample weight reached a constant value, at a relative humidity less than 1%.

The sorption/desorption isotherms recorded in these circumstances are shown in Fig.8.

The reference sample (the linen fibrous support – yarn - unfunctionalized) has a smaller sorption capacity compared to that of Sample 6 and Sample 5. High values of water vapors sorption capacity for the two last samples prove the fact that the material surface becomes more hydrophilic, more porous, respectively as it could be observed from hysteresis shape.
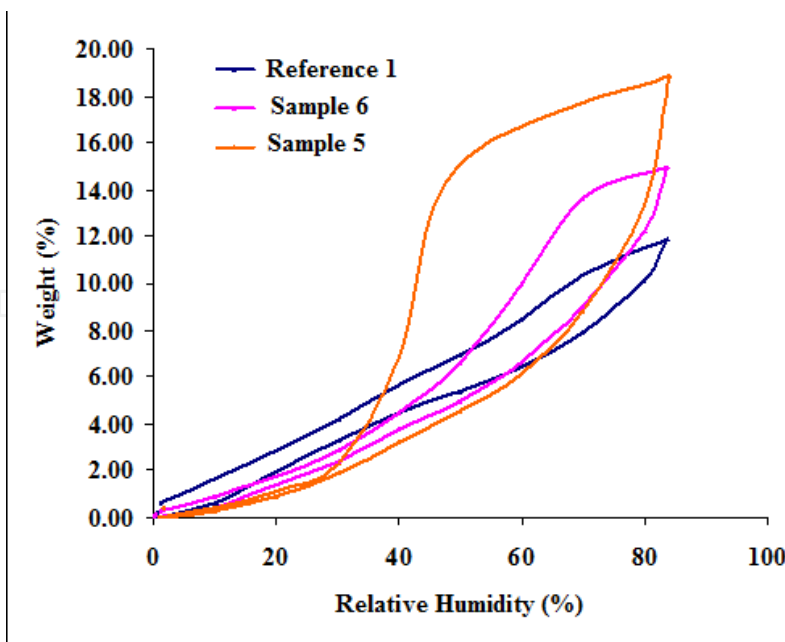
Reference 1; Sample 5; Sample 6 [10]

Figure 8. Comparative plots of rapid isotherms for water vapors sorption for the studied samples:

One of the main objectives of this review was to stress the adsorptive attributes, taking into account the improving of ZnO synthesis conditions. Consequently, the role of P123 in the ZnO synthesis was to obtain a composite with a higher porosity, in order to achieve the surface hydrophilicity, since there is direct correlation between porosity and hydrophilicity [36].

The shape of the moisture sorption isotherms for those two compounds is similar to those characteristic of mesoporous materials (type IV, according to IUPAC classification – with low sorption at low water vapor sorption (adsorption/desorption), moderate sorption at average humidity and rapidly increasing water sorption at high humidity). This type of isotherm describes the sorption behavior of hydrophilic material [37]. When a material is exposed to environmental water vapors, the water molecules firstly react with surface polar groups and form a molecular monolayer.

Based on the sorption studies, the IGAsorp software allows an evaluation of both monolayer and surface area value, by using BET (Brunauer-Emmett-Teller) model (Tabel 2).

Sample	Sorption capacity (%d.b.)	BET analysis	
		A_{BET} (m²/g)	Monolayer (g/g)
Reference 1	11.89	157.010	0.044
Sample 6	14.93	213.99	0.060
Sample 5	18.89	321.39	0.091

Table 3. The main parameters of (water vapors) sorption-desorption isotherms for the studied samples

BET (1) equation is very often used for modeling of the sorption isotherms:

$$W = \frac{W_m \cdot C \cdot RH}{(1 - RH) \cdot (1 - RH + C \cdot RH)} \tag{2}$$

where:

W- the weight of adsorbed water, Wm- the weight of water forming a monolayer, C – the sorption constant, p/po=RH- the relative humidity.

The sorption isotherms described by BET model up to a relative humidity of 40% are in relation to the sorption isotherm and material type. This method is mainly limited for II type isotherms, but can describe the isotherms of I, III and IV type [38-40], as well. The increasing water sorption is reflected both by the augmentation of monolayer and surface area values calculated with BET model (Tabel 3).

In Figure 8 the kinetic curves for humidity (water vapors) sorption/desorption processes for two of the samples are displayed. It is noticed that the time necessary for equilibrium setting for sorption processes is bigger than that of desorption. Sorption rate is smaller than that of desorption.

In Table 4 the dynamic moisture sorption capacity calculation was made using the equation written below, after the samples was kept at RH=90%, until the mass became constant:

Sorption capacity at RH=90% (%) $= \dfrac{W_{RH=90} - W_{RH=0}}{W_{RH=0}} \cdot 100$

As can be observed the obtained values are larger than those in the isotherms, this demonstrates the time necessary for reaching the equilibrium sorption is longer.

Sample	Weight at RH=0% (mg)	Weight at RH=90% (mg)	Sorption dynamic capacity RH=90% (%)	Time (s)	Sorption rate ($\cdot 10^{-3}$ %/s)
Reference 1	4.58	5.14	12.28	32	3.82
Sample 6	5.32	6.34	19.14	50	3.75
Sample 5	5.56	6.83	22.77	40	5.58

Table 4. Water vapor sorption capacity and speed for a longer time (until sample weight remains constant at a relative humidity of 90%)

In case of sample 5, the DVS analysis were made at two temperatures (25 °C and 35 °C), and the influence of this parameter on the sorption/desorption isotherms and kinetics are presented in Figure 8 and Figure 9 respectivelly.
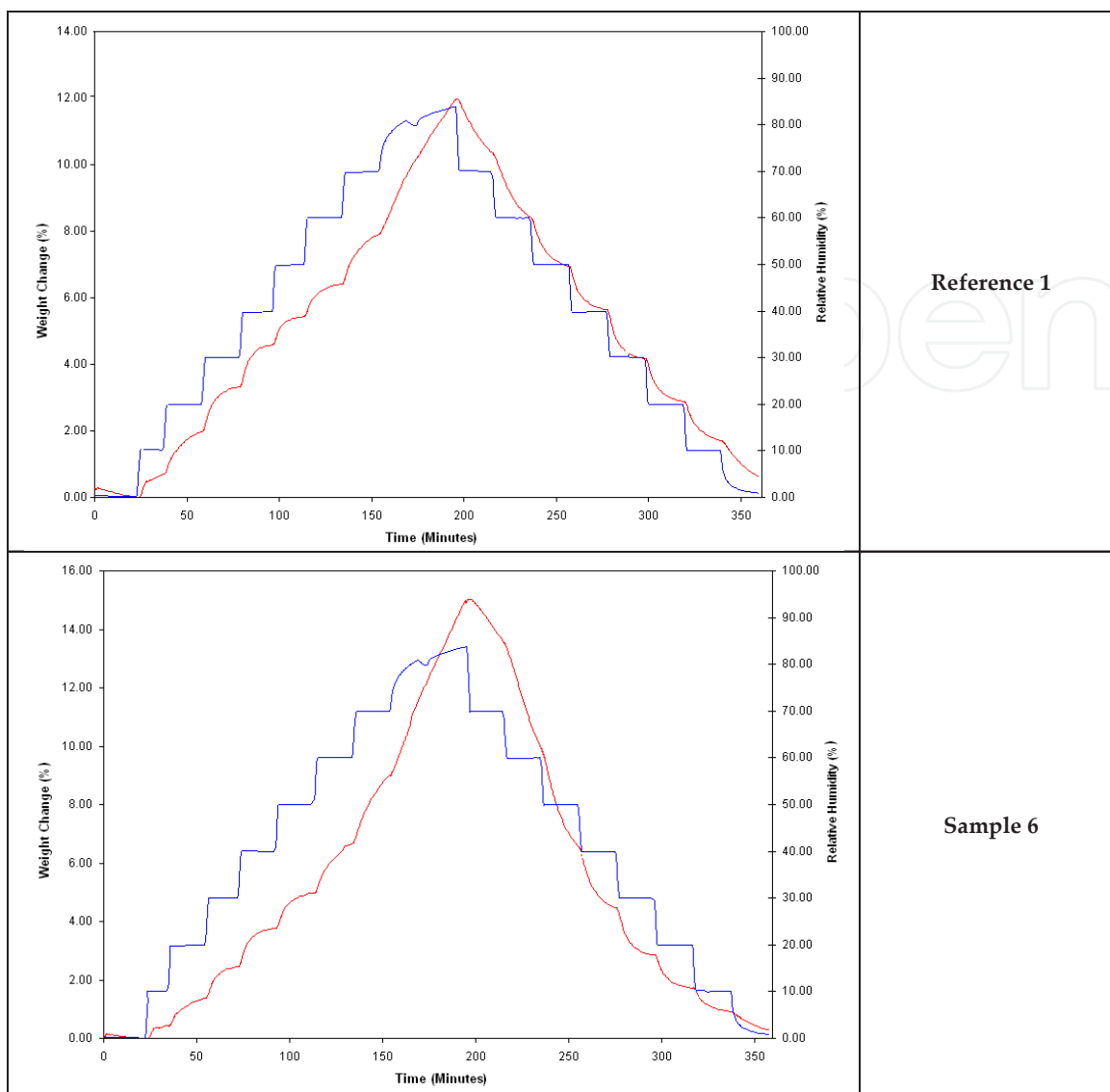
Reference 1; Sample 6 [10]

Figure 9. Kinetic curves for sorption/desorption processes of water vapors in the studied samples

From Table 5, it is noticeable the augmentation of temperature conducts to an increase on vapor sorption capacity of the sample (probably due to the hydrogen bonds formation favoring sorption).

Sample	Sorption capacity (%)
Sample 5_25	18.89
Sample 5_35	31.59

Table 5. Water vapor sorption capacity for sample 5 at both 25 °C and 35 °C respectively
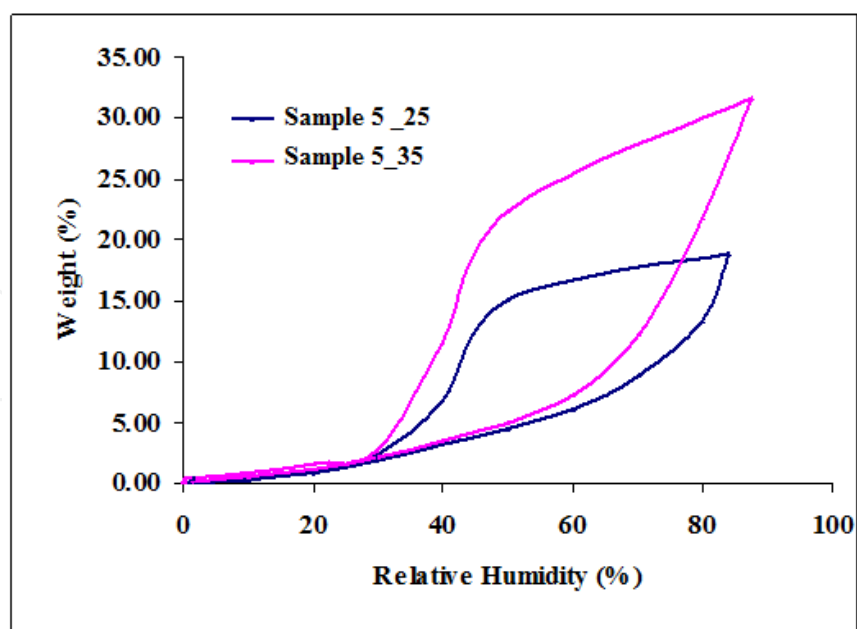
Figure 10. Comparative plots of rapid water vapors sorption/desorption isotherms for sample 5 [10] at both 25 °C and 35 °C respectively

The differences between sorption-desorption speeds of those two temperatures for Sample 5 indexed sample are clearly highlighted by the presence of modified hysteresis and also by the kinetics curves.

3.2. Thermal degradation mechanism of linen fibrous supports treated with ZnO

Considerable attention has been devoted to complete or correlate the results provided by the XRD analysis, with the DSC studies, since the last type of investigation is able to evaluate the crystallization/melting processes.

Vrinceanu et al tested thermal attributes of fibrous supports - ZnO nanocomposites under nitrogen [41] The DSC curves of are shown in figures above.

In the range 370°-395°C, in a typical DSC curve of cellulosic fibres, there is an endothermic peak, which has been shown to be primarily due to the production of laevoglucosan [42].

For linen fibres, this peak is sometimes partly or completely marked by an exothermal effect around 340°C, attributed to a base-catalysed-dehydration reaction that takes place in the presence of alkaline ions, such as those of sodium [43].

From 200 to 250°C a progressive mass loss associated with water release was observed. From the literature it is well known that lignocellulosic fibers degrade in several steps; the cellulose degrades between 310°–360°C, whereas the hemicellulose degrades at about 240°–310°C, and the lignin has been shown to degrade in wide temperature interval (200°–550°C) [44]. Technically speaking, it is not possible to separate the different degradation processes of the fiber components because the reactions are very complex and overlap in the range of 220°–360°C. It is noteworthy that the nanocomposite treated with ZnO nanoparticles with the assistance of
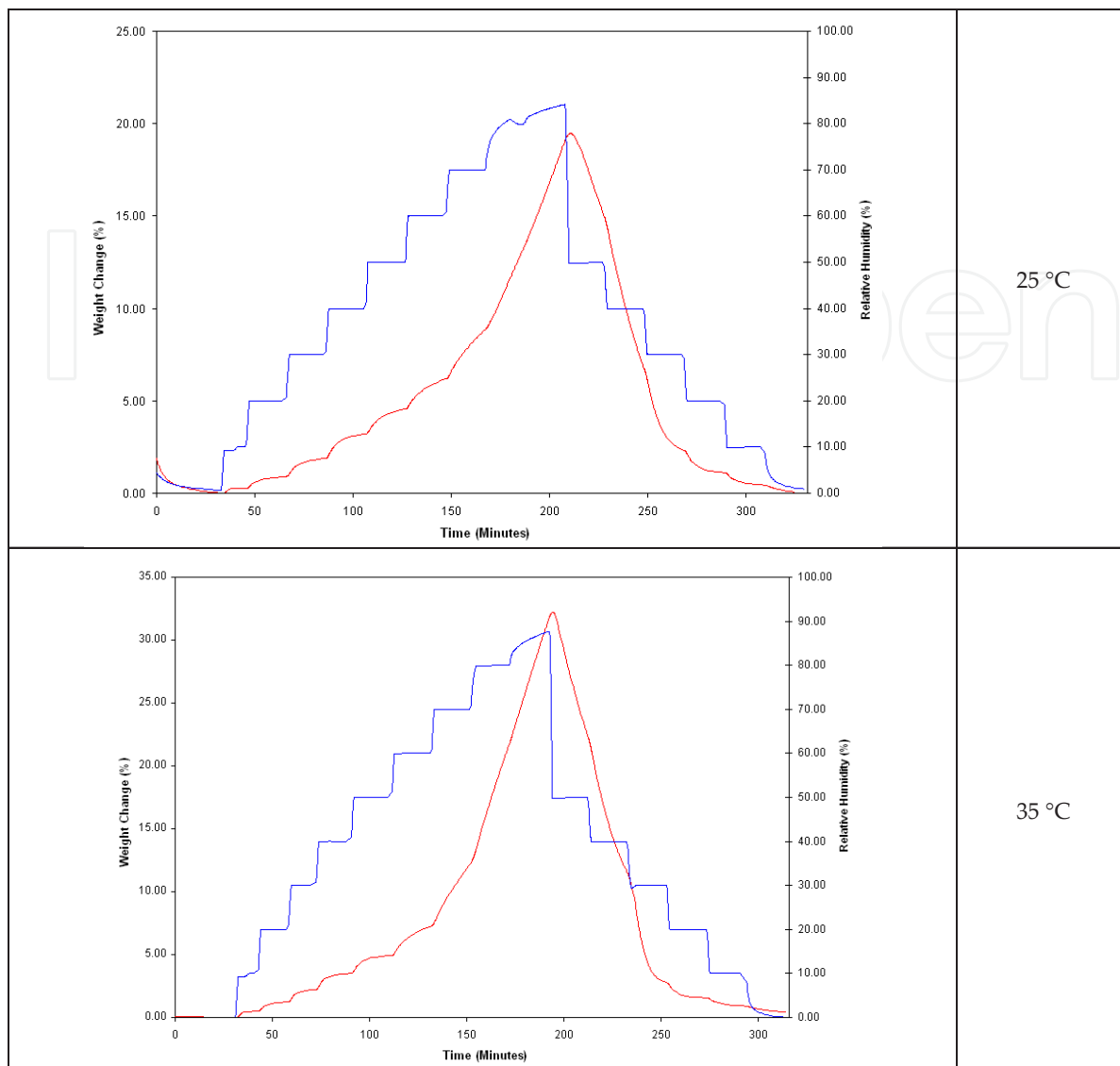
Figure 11. Kinetic curves for sorption/desorption processes of water vapors for sample 5 at both 25 °C and 35 °C respectively [10]

MCT started to decompose at higher temperature than sample treated in the same conditions but without the presence of zinc oxide. Nevertheless, the existence of the MCT on the surface of the probes delayed the thermal degradation of the fibrous linen samples, even the non-treated with the zinc oxide particles.

It can be claimed that cellulose is thermally decomposed through two types of reactions. At lower temperatures, there is a complex process of gradual degradation including dehydration, depolymerisation, oxidation, evolution of carbon monoxide and carbon dioxide, and formation of carbonyl and carboxyl groups, ultimately resulting in a carbonaceous residue forms.

The endothermic band around 260°C from DSC curves (Fig. 14 (a) and (b)) indicates a weight loss. The surface acidity of zinc oxide nanoparticles keeps accelerating the decomposition of
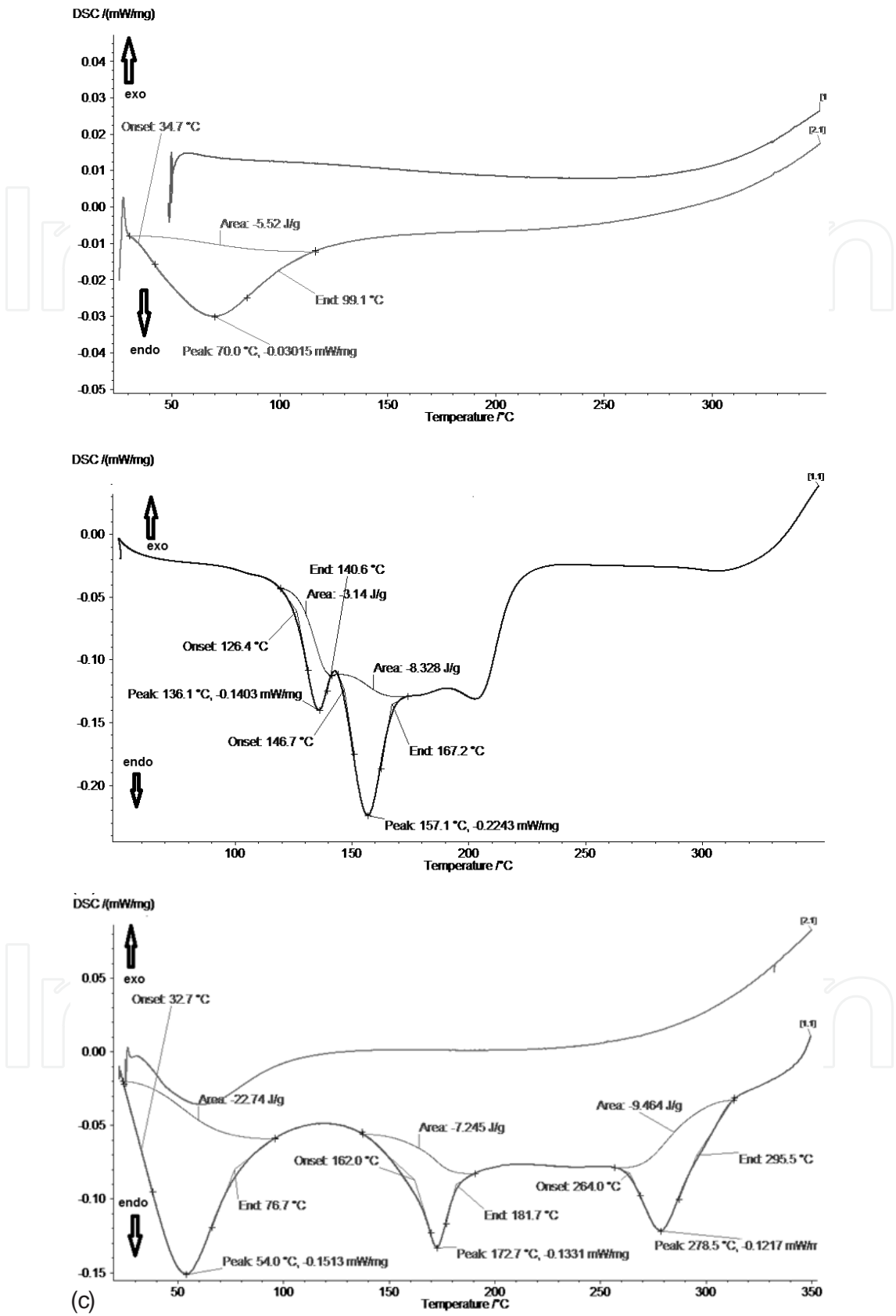
Figure 12. Typical DSC curve under nitrogen for: a Sample 3; b Sample 4; c. Sample 5 [41]
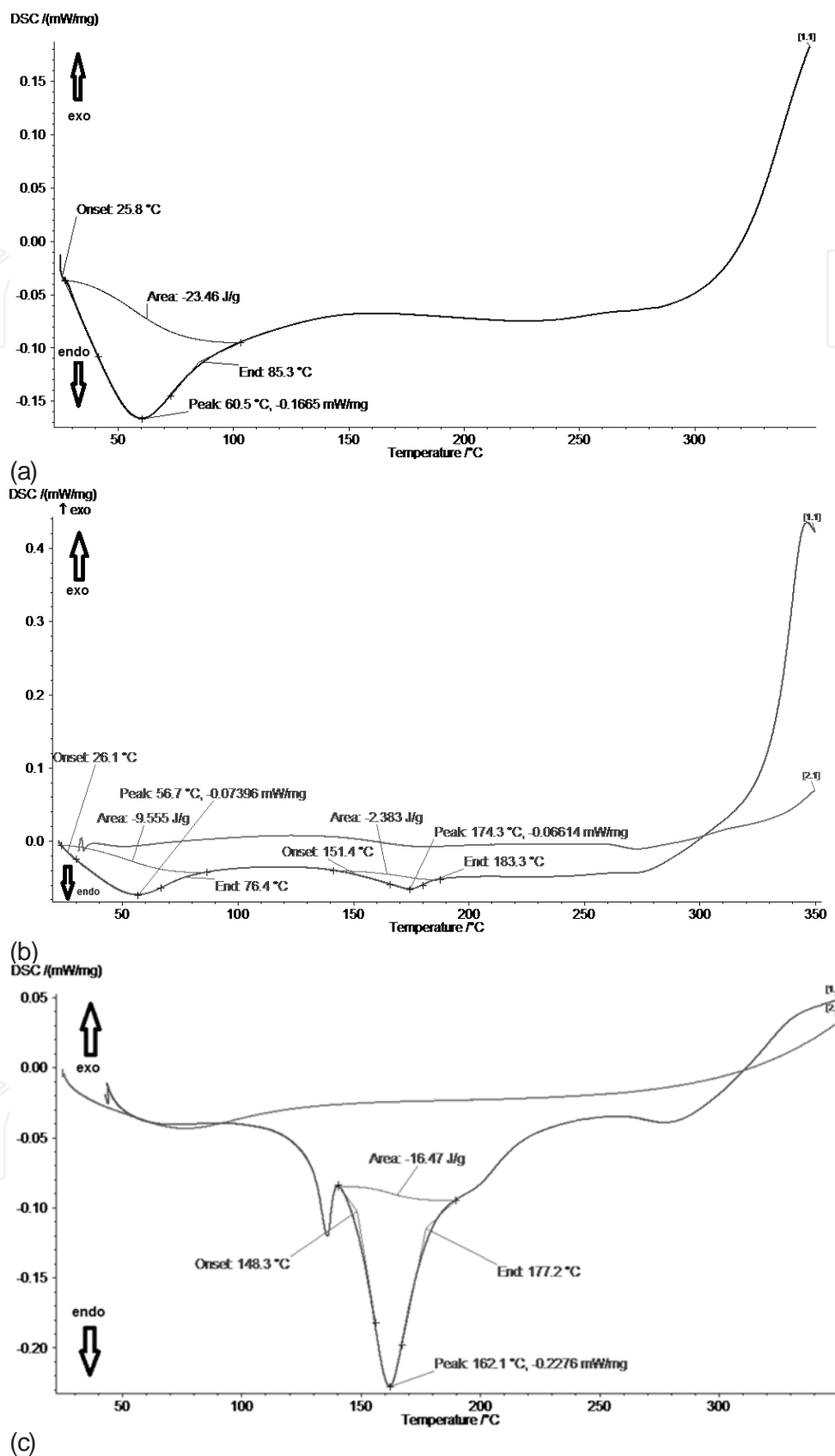
Figure 13. Typical DSC curve under nitrogen for: a – Sample 4; b – Sample 5; c – Sample 6 [41]

the fibrous substrate, as the temperature rises to 310°C, According to the FTIR spectra, a very much lower amount of carbonyl groups is found in the linen - ZnO nanocomposite specimens.

Meanwhile, MCT having a higher thermal conductivity as well as a greater heat capacity value absorbs the heat transmitted from the surroundings and retard the direct thermal impact to the polymer backbone [45,46]. As a consequence, zinc oxide stabilizes the polymer molecules of the underneath substrates and delays the occurrence of major cracking up to 400°C (Fig. 15).

The masking effect of an exothermal reaction on the endothermic cellulose decomposition was clearly highlighted by the behavior of the reference fibrous linen (non-functionalized) subjected to the thermal treatment in N_2; it shows an exothermal peak at 260°C with a decreased enthalpy after the thermal treatment; the exothermal effect is attributable to β-cellulose decomposition as observed in a curve of a cotton sample. Surprisingly, even within the second cycle of thermal treatment, the sample exhibits a similar exothermal peak at 363°C.

4. Summary and outlook

The review has been focused on a series of MCT-β-CD grafted linen fibrous support (yarn) in whose matrices zinc oxide nanoparticles have been introduced with the assistance of two different surfactants. The coating particles fell off easily for the ZnO powder hydrothermally synthesized without any surfactant assistance after washing, which might have been caused by the weak attaching force (coordinated bond between ZnO and linen) induced by the deteriorated crystallinity.

Wetting characteristics are influenced by the type of surfactant used during the hydrothermal synthesis. It is in direct implication onto the relationship between the morphological, structural and chemical attributes and water vapor sorption-desorption behavior. Hydrophilicity of these fibrous composites has increased and based on the sorption/desorption isotherms registered by DSV, BET surface area, as well as XRD measurements were estimated, and assimilated these fibrous composites, set by IUPAC, with mesoporous materials. Humidity loss and drying speed of water from these studied samples depend of the type of surfactant.) A quantification of samples, in terms of their thermal stability has been surveyed, as well. Thus, this paper review intends to develop an innovative and more appropriate synthetic procedure and characterization of nanoscale ZnO coated fibrous composites under favourable conditions, by using the synergic effect of MCT and CTAB/P123 as surfactants. Prominent assessed attributes were emphasized:

- thermal stability and degradation mechanism of ZnO nanocoated linen fibrous samples;

- Cumulative barrier attributes conferred by the new components that interfered in the preparation technique: CTAB/P123 and MCT

These new features are believed to be the promising new lines of exploration of nanoscale ZnO coated fibrous composites in textile area.

Acknowledgements

Author details

Narcisa Vrinceanu[1,2], Alina Brindusa Petre[1], Claudia Mihaela Hristodor[1], Eveline Popovici[3], Aurel Pui[1], Diana Coman[2] and Diana Tanasa[1]

1 "Al.I.Cuza" University of Iasi, Iasi, Romania

2 "L.Blaga" University of Sibiu, Romania

3 Al.I.Cuza" University of Iasi, Faculty of Chemistry, Departament of Materials Chemistry, Romania

References

[1] Weber, J., Futterer, C., Gowri, V.S., Attia, R., Viovy, J.L., La Houille Blanche 5:40 (2006); Saxana, M, Gowri. V.S., J Polym Compd 24:428 (2003); Gowri, V.S., Saxena, MJ Chem Technol 14:145 (1997)

[2] Raveendran, P., Fu, J., Wallen, S.L., Completely ''green'' synthesis and stabilization of metal nanoparticles, J. Am. Chem. Soc. 125, 13940–13941 (2003)

[3] Mucalo, M.R., Bullen, C.R., Arabinogalactan from the Western larch tree: a new, purified and highly water-soluble polysaccharide-based protecting agent for maintaining precious metal nanoparticles in colloidal suspension, J. Mater.Sci. 37, 493–504 (2002)

[4] He, J.H., Kunitake, T., Nakao, A., Facile in situ synthesis of noble metal nanoparticles in porous cellulose fibers, Chem. Mater. 15, 4401–4406 (2003)

[5] He, J.H., Kunitake, T., Nakao, A., Facile fabrication of composites of platinum nanoparticles and amorphous carbon films by catalyzed carbonization of cellulose fibers, Chem. Commun. 4, 410–411 (2004)

[6] Walsh, D., Arcelli, L., Ikoma, T., Tanaka, J., Mann, S., Dextran templating for the synthesis of metallic and metal oxide sponges, Nat. Mater. 2, 386–390 (2003)

[7]   Vigneshwaran, N., Kumar, S., Kathe, A.A., Varadarajan, P.V., Prasad, V., Functional finishing of cotton fabrics using zinc oxide–soluble starch nanocomposites, Nanotechnology 17, 5087–5095 (2006)

[8]   Ma, X.F., Chang, P.R., Yang, J.W., Yu, J.G.,. Preparation and properties of glycerol plasticized-pea starch/zinc oxide–starch bionanocomposites, Carbohydr. Polym. 75, 472–478 (2009)

[9]   Radhakrishnan, T., Georges, M.K., Nair, P.S., 2007. Study of sago starch–CdS nanocomposite films: Fabrication, structure, optical and thermal properties, J.Nanosci. Nanotechnol. 7, 986–993 (2007)

[10] Diana Tanasa, Narcisa Vrinceanu, Alexandra Nistor,Claudia Mihaela Hristodor, Eveline Popovici, Ionut Lucian Bistricianu, Florin Brinza1, Daniela-Lucia Chicet,Diana Coman, Aurel Pui, Ana Maria Grigoriu, Gianina Broasca, Zinc oxide-linen fibrous composites: nmorphological, structural, chemical and humidity adsorptive attributes, Textile Research Journal, 82(8) 832–844 (2012)

[11] Chandramouleeswaran, S., Mhaskel, S., Kathe, A.A., Varadarajan, P.V., Prasad, V., Vigneshwaran, N., Functional behaviour of polypropylene/ZnO–soluble starch nanocomposites, Nanotechnology 18, 385702 (2007)

[12] Tang Z K, Wong G K L, Yu P, Kawasaki M, Ohtomo A, Koinuma H and Segawa Y Appl. Phys. Lett. 72 3270 (1998)

[13] Corrales T, Catalina F, Peinado C, Allen NS, Fontan E. Photooxidative and thermal degradation of polyethylenes interrelationship by chemiluminescence, thermal gravimetric analysis and FTIR data. J Photochem Photobiol. A 2002;147:213-24

[14] Gawas UB, Verenkar VMS, Mojumdar SC. Synthesis and characterization of Co0.8Zn0.2Fe2O4 nanoparticles. J Therm Anal Calorim. 2011;104:879-883.

[15] Gonsalves LR, Mojumdar SC, Verenkar VMS. Synthesis and characterization of Co0.8Zn0.2Fe2O4 nanoparticles. J Therm Anal Calorim. 2011;104:869-873

[16] Gonsalves LR, Mojumdar SC, Verenkar VMS. Synthesis of cobalt nickel ferrite nanoparticles via autocatalytic decomposition of the precursor. J Therm Anal Calorim. 2010;100:789-792.

[17] Gawas UB, Mojumdar SC, Verenkar VMS. Synthesis of cobalt nickel ferrite nanoparticles via autocatalytic decomposition of the precursor. J Therm Anal Calorim. 2010;100:867-871.

[18] Verdu J, Rychly J, Audouin L. Polym Degrad Stab. 2003;79:503-9.

[19] Allen NS, Edge M, Corrales T, Childs A, Liauw CM, Catalina F, et al. Ageing and stabilization of filled polymers: an overview. Polym Degrad Stab. 1998;61:183-99.

[20] Mojumdar SC, Moresoli C, Simon LC. Legge RL. Edible wheat gluten (WG) protein films: Preparation, thermal, mechanical and spectral properties. J Therm Anal Calorim. 2011; 104:929-936.

[21] Gawas UB, Mojumdar SC, Verenkar VMS. J Therm Anal Calorim. 2009;96:49-52

[22] Mocanu AM, Odochian L, Apostolescu N, TG-FTIR study on thermal degradation in air of some new diazoaminoderivatives. J Thermal Anal Calorim. 2010;100 (2): 615-622.

[23] Singhal M, Chhabra V, Kang P, Shah DO. Mater Res Bull. 1997; 32:239-247

[24] Hingorani S, Pillai V, Kumar P, Multani MS, Shah DO. Mater Res Bull. 1993; 28:1303-1310.

[25] Fan Q, John J, Ugbolue SC, Wilson AR, Dar YS, Yang Y. AATCC Rev. 2003; 3(6):25.

[26] Grigoriu A.M., Cercetări în domeniul compusilor de incluziune ai ciclodextrinelor si al derivatilor acestora cu aplicatii în industria textilă. Ph. D. Diss., Iasi (2009)

[27] Reuscher H, Hinsenkorn R. BETA W7 MCT-new ways in surface modification. J Incl Phenom Macrocycl. 1996;25:191–196.

[28] Ogata N, Ogawa T, Ida T, Yanagawa T, Ogihara T, Yamashita A. Sen'i Gakkaishi. 1995;51(9), 439.

[29] Patterson A. The Scherrer Formula for I-Ray Particle Size Determination. Phys Rev. 1939;56 (10): 978–982.

[30] Xiao-Juan J, Pascal Kamdem D. Chemical composition crystallinity and crystallite cellulose size in populus hybrids and aspen. Cellul Chem Technol. 2009;43(7-8): 229-234

[31] Reuscher H., Hinsenkorn R., Journal of inclusion phenomena and macrocyclic chemistry, 25, 191–196 (1996)

[32] Taubert, A., Wegner, G., Formation of uniform and monodisperse zincite crystals in the presence of soluble starch. J. Mater. Chem. 12, 805–807 (2002)

[33] J. Yu et al. Bioresource Technology 100 2832–2841 (2009)

[34] Sunkyu Park1,3, John O Baker1, Michael E Himmel1, Philip A Parilla and David K Johnson, Cellu lose crystallinity index: measurement techniques and their impact on interpreting cellulase performance, Biotechnology for Biofuels 2010, 3:10 Jiugao, Yu, Jingwen, Yang, Baoxiang, Liu, Xiaofei, Ma, Preparation and characterization of glycerol plasticized-pea starch/ZnO–carboxymethylcellulose sodium nanocomposites, Bioresource Technology 100, 2832–2841 (2009)

[35] Gu, F., Wang, S.F., Lu, M.K., Zhou, G.J., Xu, D., Yuan, D.R. Langmuir, 20: 3528 (2004)

[36] http://test.ttri.org.tw/neweng/RD/images/pub3.pdf

[37]   Brunauer, S., Deming, L.S., Deming, W.E., Teller, E. On a Theory of the van der Waals adsorption of gases, J Am Chem Soc, 62(7): 1723-1732 (1940

[38]   Guggenheim, E. A. Application of Statistical Mechanics, Clarendon Press, Oxford, 186-206 (1966).

[39]   Anderson, R.B. Modifications of the Brunauer, Emmett and Teller Equation, J Am Chem Soc, 68(4): 686-691 (1946)

[40]   de Boer, J.H. The Dynamical Character of Adsorption, 2nd ed., Clarendon Press, Oxford, 200-219 (1968).

[41]   Vrinceanu , N., Tanasa, D., Hristodor C.M., Brinza, F., Popovici E., Gherca D., Pui A., Coman, D., Carsmariu A., Bistricianu I., Broasca, G., Synthesis and characterization of zinc oxide nanoparticles Application to textiles as thermal barriers, J Therm Anal Calorim, DOI 10.1007/s10973-012-2269-7 (2012)

[42]   Ye DY, Farriol X. Preparation and characterization of methylcellulose from Miscanthus Sinensis. Cellul. 2005; 12, 507.

[43]   Revola JF, Dietricha ND D, Goring AI. Effect of mercerization on the crystallite size and crystallinity index in cellulose from different sources. Can J Chem. 1987;65, 1724.

[44]   [44].Nevell TP, Zeronian S H. Cellulose Chemistry and Its Applications M. Chichester: Ellis Horwood Ltd., 1985;423–454.

[45]   Lee HJ, Yeo SY, Jeong SH. Antibacterial Effect of Nanosized Silver Colloidal Solution on Textile Fabrics. J Mater Sci. 2003;38:2199–2204.

[46]   Riva A, Algaba IM, Montserrat P. Action of a finishing product in the improvement of the ultraviolet protection provided by cotton fabrics. Modelisation of the e▪ect. Cellul. 2006;13:697–704.